Learning Science Through Research
Published by Keck Geology Consortium

Short Contributions
Keck Geology Consortium
Volume 31
May 2018

PRELIMINARY WAVELET ANALYSIS OF CIRCUM-ANTARCTIC ODP WELL LOGS AND SPLIT-CORE XRF SCANS FROM ODP SITE 697 CORES INFERS OBLIQUITY SIGNAL

ANDREW HOLLYDAY, Middlebury College
Research Advisors: Suzanne O'Connell, Will Amidon, and Joe Ortiz

ABSTRACT

Circum-Antarctic marine sediment archives in this study preserve late Pliocene and early Pleistocene depositional geochronology linked to continental erosional systems, and surface and bottom currents. Geophysical IODP/ODP down hole well logs from the Plio-Pleistocene offer the only available offshore (>100 km and ~3000 m water depth) marine sediment record for circum-Antarctic scientific ocean drilling sites. Even though recovered cores are commonly discontinuous, they can provide a higher resolution window into sedimentary process. Principal component analysis of XRF elemental counts from Weddell Sea ODP Leg 113 Site 697 split-cores reveals a dominant terrigenous elemental component, which may be linked to proximal ice erosional regimes. Wavelet analysis on both the well log and XRF datasets allows us to cross-calibrate proxies and identify 23, 41, and 100-kyr Milankovitch periodicities, with 41-kyr dominating. Wavelet analysis is also used to derive discretized linear sedimentation rates that agree with available IODP/ODP paleomagnetic and biostratigraphic age models and imply spatiotemporal changes in Antarctic depositional history. Finally, the dominating obliquity signal in these offshore marine deposits provides evidence for coupling between nearshore glacial sequence stratigraphy.

INTRODUCTION

Global geological evidence from marine and terrestrial systems has demonstrated that prior to the onset of vast northern hemisphere glaciation in the Pleistocene, early Pliocene atmospheric CO_2 levels were near 400 p.p.m.v., and global mean temperatures were approximately 3°C warmer than present (Raymo et al., 1996; Pagani et al., 2010). These conditions offer a powerful analogue in the paleoclimate record that can be used to inform modern anthropogenic warming and sea level rise. Well-dated marine lithostratigraphic constraints from the Ross Sea by the ANDRILL program have linked 40-kyr fluctuations in the ice sheet extent and sediment record to orbitally-driven cycles in solar insolation (changes in Earth's obliquity; Naish et al., 2009).

This project utilizes Ocean Drilling Program (ODP) cores from Expedition 113 in the Weddell Sea and Integrated Ocean Drilling Program (IODP) and ODP geophysical down-hole well logs from Expeditions 119 and 188 from Prydz Bay, Expedition 178 from the Bellingshausen Sea, and Expedition 318 offshore Wilkes Land to study the connection between nearshore diatomite-diamicton sequences (ANDRILL) and distal circum-Antarctic continental shelf sediments. While the ANDRILL program was able to study glacial cycles by directly identifying lithological facies diagnostic of either glacial advance or retreat, this project uses sediment cores (XRF) and borehole measurements (gamma ray and resistivity) in its analysis.

LOCALITIES

This study considers four circum-Antarctic marine ODP/ IODP locations: the Weddell Sea, Prydz Bay, the Bellingshausen Sea, and offshore Wilkes Land (see O'Connell, this volume for location map).

Expedition 113 Site 697 is located northeast of the Antarctic Peninsula in the northwestern Weddell Sea, close to where the Weddell Gyre joins the Antarctic Circumpolar Current, both of which flow clockwise. This site is approximately 800 km from the modern terminus of the Filchner-Ronne Ice Shelf, which is a primary source of sediment at this site (Bentley & Anderson, 1998).

The Pyrdz Bay ODP Sites (739, 742, and 1166) from Expeditions 119 and 188 are located approximately 110 km from the modern terminus of the Amery Ice Shelf, which is also the primary regional sediment source. All three Pyrdz Bay sites are located on the modern continental shelf.

The Bellingshausen Sea ODP Sites (1095, 1096, and 1103) from Expedition 178 are located 400 km to the west of the Antarctic Peninsula. These sites are dominated by erosional input from the proximal Transantarctic Mountains via paleo-ice streams (Barker, Camerlenghi, &Acton, 1999).

The Wilkes Land IODP sites (U1359 and U1360) are located to the west of the Ross Sea along the Wilkes and Adelie coasts. Sediment delivered to these sites, which are located approximately 200 km offshore, is sourced from the East Antarctic Ice Sheet (Verma et al., 2014).

DATA COLLECTION

High resolution *in situ* x-ray fluorescence (XRF) intensities were collected for 22 major and trace elements on Expedition 113 Site 697 split cores at the International Ocean Discovery Program (IODP) facility in College Station, TX using an Avaatech XRF Core Scanner with Brightspec silicon drift detectors (SDD). Spot measurements (spot size ~1 cm^2) were analyzed every 2 cm along the cores for 10, 30, and 50 kVp energy profiles. A peak area integration and background model was developed and the data were processed using bAxil.

ANALYSIS OF WELL LOGS AND XRF SCANS

Principal component analysis (PCA) with varimax rotation and Kaiser normalization, which is a statistical technique that uses orthogonal transformation to isolate linearly uncorrelated components, was performed on the continuous segments of the XRF elemental counts dataset (3H-4H, 8H, 14X-15X, and 19X-20X) from Hole 697B from the Weddell Sea using SPSS. This analysis produces a dominant component that explains approximately 35% of variance across the distribution (Fig. 1). PCA shows that Mg, Al, Si, K, Ti, Fe, Ga, Rb, Zr, Ni, and Ag systematically explain the majority of variance within this component which

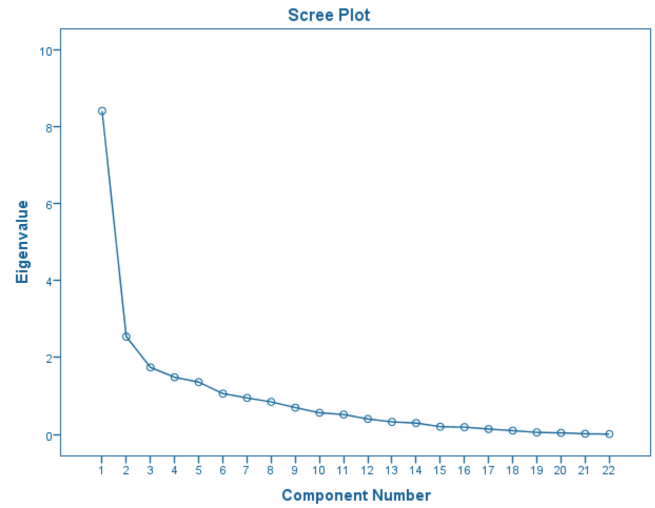

Figure 1: Principal Component Analysis (PCA) scree plot of component numbers versus eigenvalues indicating clear orthogonally-independent Component 1, which explains ~35% of the variability of the entire dataset and is dominantly explained by Mg, Al, Si, K, Ti, Fe, Ga, Rb, Zr, Ni, and Ag input variables. These elements correspond to terrigenous sediment input, which is analyzed with wavelet analysis.

The dominant PCA terrigenous component scores were then analyzed using wavelet code developed at the University of Colorado, Boulder using Interactive Data Language (IDL). The code first detrends the data with a third-degree polynomial, then uses the Mortlet wavelet and Fourier transformations to decompose time series into time-frequency phase space, and ultimately deconvolves cycles recorded in the stratigraphy (Fig. 2; Torrence & Compo, 1998). Only continuous segments of Site 697, Weddell Sea cores were selected in order to avoid coring unconformities which violate fundamental assumptions within wavelet analysis methodology. In this analysis, the recovered sections are conformable. In order to capture the 100-kyr periodicity, a minimum of 1000 centimeters—an overestimate given speculated sedimentation rates during the Pliocene—was run through wavelet analysis. Down hole geophysical well log datasets including gamma ray spectrometry and dual-induction resistivity from Prydz Bay, the Bellingshausen Sea, and off shore Wilkes Land were analyzed with the same wavelet code.

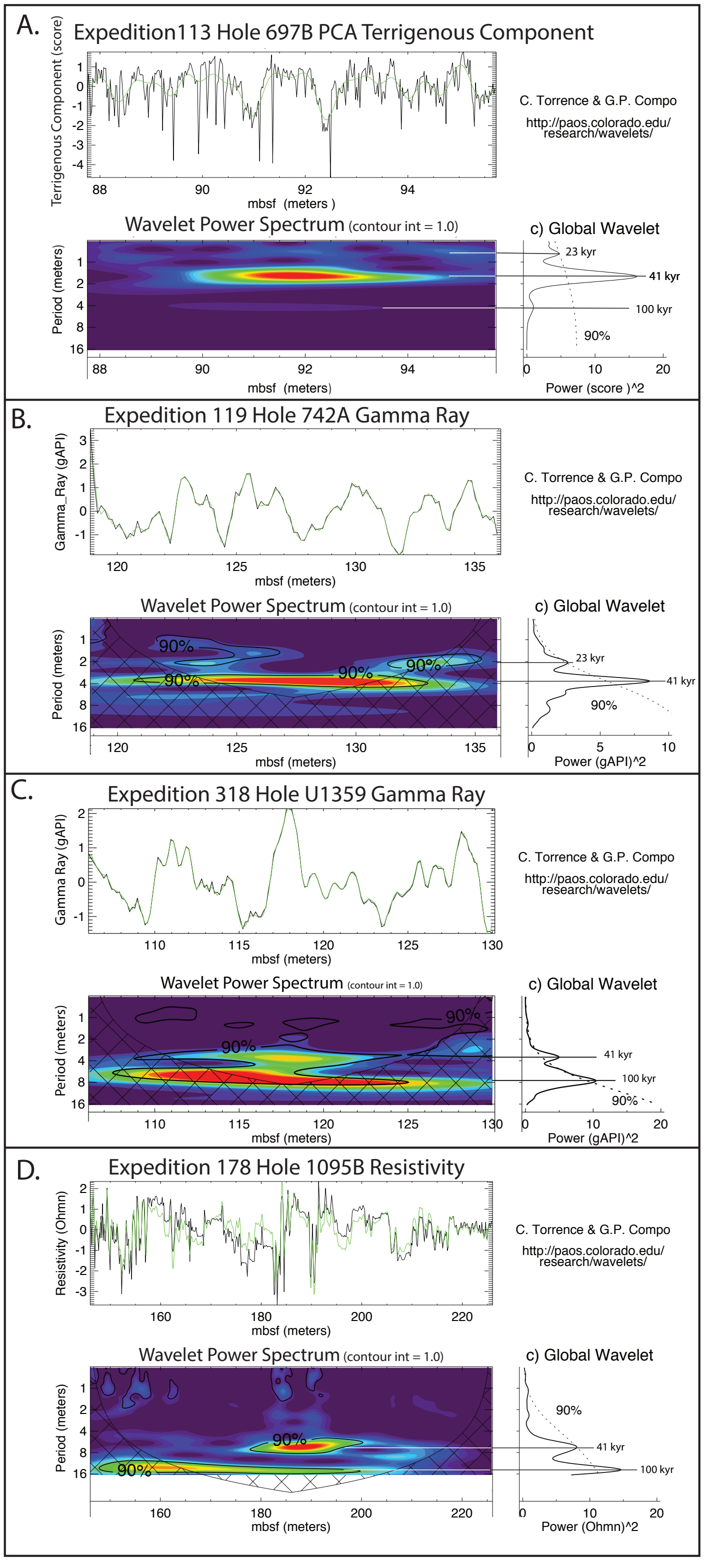

Figure 2: Wavelet analyses of circum-Antarctic sediment archives from ODP/IODP Expeditions 113, 119, 318, and 178. Raw and detrended (green) datasets (PCA component, gamma ray, and resistivity) versus meters below sea floor (mbsf). A: PCA terrigenous component from XRF core measurements from Expedition 113 in the Weddell Sea, Hole 697B Core 8H. This late Pliocene segment extends 7.9 meters, and according to internal (wavelet) age control represents >190-kyrs of deposition. Milankovitch assigned periodicities show dominant 41-kyr signal in Global Wavelet. B: Gamma Ray well-log from Expedition 119 in Prydz Bay from well-logging. This Pliocene segment extends 17.07 meters, and according to internal (wavelet) age control, represents >187-kyrs of deposition. A 41-kyr assigned periodicity dominates the Global Wavelet. C: Gamma Ray well-log from Expedition 318, Hole U1359, offshore of Wilkes Land from post coring logging. This early Pliocene segment extends 23.91 meters, and according to internal (wavelet) and external (biostratigraphic and paleomagnetic) age control, represents between 359-kyrs (internal) and 543-kyrs (external) of deposition. This record is dominated by the 41-kyr obliquity periodicity, with an insignificant 100-kyr signal that is primarily contained within the cone of influence. D: Resistivity well-log from Expedition 178 Hole 1095B in the Bellinghausen Sea from post coring logging. This early Pliocene segment extends 79.85 meters, and according to internal (wavelet) and external (biostratigraphic and paleomagnetic) age control, represents 505-kyrs (internal) to 1.3-Ma (external). This resistivity archive shows dominant 41-kyr and 100-kyr periodicities, but the 100-kyr is mostly contained in the cone of influence, which indicates it should be rejected. Overall, the geophysical well-log wavelet signal is more ambiguous from the Bellinghausen Sea, which may be a function of more complex sedimentary mechanisms (Scheuer et al., 2006).

RESULTS

Milankovitch orbital periods (23, 41, and 100 kyrs) were assigned to zones of significantly elevated power scores on the Global Wavelet, which translates frequencies in space to frequencies in time with the ultimate goal of deriving linear sedimentation rates (Table 1; True-Alcala, 2015). For most datasets, all three Milankovitch periodicities are visible and statistically significant. Sedimentation rates agree across periodicities (maximum standard deviation of 3.3 cm/kyr), which suggests assignments are correct. In Weddell Sea Hole 697B, the 41-kyr assigned obliquity signal primarily dominates during the Pliocene (Fig. 2A) with some exceptions where the dominant Global Wavelet signal is 100-kyr (eccentricity); these analyses are within the cone of influence, which may suggest the signal is an artifact of a padding feature in the code designed to remove edge effects. Prydz Bay well logs show the most dominant 41-kyr signal, while the Bellingshausen Sea and offshore Wilkes Land well-logs (Fig. 2C-D) show greater ambiguity between obliquity and eccentricity.

Derived circum-Antarctic sedimentation rates agree within an order of magnitude with a standard deviation of 3.6 cm/kyr. Weddell Sea sedimentation rates agree within core segments and range from approximately 4.0 to 7.6 cm/kyr; variability is likely a function of temporal (stratigraphic) sedimentation variation. In Prydz Bay, derived sedimentation rates range from 8.5 to 15.0 cm/kyr; Wilkes Land sedimentation rates are also within range with 6.7 to 9.4 cm/kyr. Lastly, Bellingshausen Sea derived rates range from 5.1 to 15.7 cm/kyr (Table 1).

DISCUSSION

This preliminary wavelet analysis of terrigenous component XRF data and geophysical well log measurements from circum-Antarctic sites demonstrates that offshore (>100 km and ~3000 m deep) marine sediments from the Pliocene record obliquity-paced deposition from continental erosion. While the ANDRILL program shows clear nearshore glacial sequence stratigraphy driven by obliquity during the Pliocene, IODP/ODP offshore cores and wells logs provide evidence for depositional obliquity signals as far as 800 km from the sediment source (Naish et al., 2009). The geographic diversity of IODP/ ODP sites can also inform spatiotemporal changes in ice volume. Obliquity dominates in each study region presented here, except in the Bellingshausen Sea, where local sedimentary mechanisms and architecture may obfuscate the signal (Scheuer et al., 2006). Scheuer et al. (2006) suggests that despite clear ice sheet sediment contribution during the Pliocene, bottom currents also had a significant influence on Bellingshausen Sea depocenters, which may explain ambiguity between obliquity and eccentricity-dominated wavelet analysis.

Otherwise, the Weddell Sea, Prydz Bay, and Wilkes Land sites show consistent obliquity-driven sedimentation (Fig. 2B). The Prydz Bay sites—the most nearshore locality presented—show the most decisive wavelet signal compared to more offshore circum-Antarctic study localities. This agrees with Hambrey

Locality	Dataset	Orbital Cycle (kyr)	Length (cm)	Sedimentation Rate (cm/kyr)
Weddell Sea	XRF Site 697 3-4H	23	180	7.82
Weddell Sea	XRF Site 697 3-4H	100	700	7
Weddell Sea	XRF Site 697 8H	23	80	3.47
Weddell Sea	XRF Site 697 8H	41	180	4.39
Weddell Sea	XRF Site 697 8H	100	430	4.3
Weddell Sea	XRF Site 697 14X	23	100	4.34
Weddell Sea	XRF Site 697 14X	41	220	5.36
Weddell Sea	XRF Site 697 14X	100	480	4.8
Weddell Sea	XRF Site 697 19X	23	180	7.82
Weddell Sea	XRF Site 697 19X	41	320	7.8
Weddell Sea	XRF Site 697 19X	100	710	7.1
Prydz Bay	Gamma Ray 1166A	23	290	12.6
Prydz Bay	Gamma Ray 1166A	41	710	17.31
Prydz Bay	Gamma Ray 739C	23	180	7.82
Prydz Bay	Gamma Ray 739C	41	380	9.26
Prydz Bay	Gamma Ray 742A	23	200	8.69
Prydz Bay	Gamma Ray 742A	41	390	9.51
Bellingshausen Sea	Resistivity 1103A	41	310	7.56
Bellingshausen Sea	Resistivity 1103A	100	900	9
Bellingshausen Sea	Gamma Ray 1095B	41	200	4.87
Bellingshausen Sea	Gamma Ray 1095B	100	540	5.4
Bellingshausen Sea	Resistivity 1095B	41	700	17.07
Bellingshausen Sea	Resistivity 1095B	100	1450	14.5
Wilkes Land	Gamma Ray U1359D	41	300	7.317073171
Wilkes Land	Gamma Ray U1359D	100	600	6
Wilkes Land	Gamma Ray U1361A	41	400	9.756097561
Wilkes Land	Gamma Ray U1361A	100	900	9

Table 1: Discretized linear sedimentation rates derived according to assigned Milankovitch periodicities from wavelet analysis. Approximate agreement across orbital cycle assignments within each dataset suggests robust assignment. Variability across datasets implies spatiotemporal differences in sedimentation rate for circum-Antarctic Pliocene localities.

et al. (1991) who indicates ice advance and retreat cycles strongly influence sediment mobilization and transport from the Amery Ice Shelf. While sediment from the Weddell Sea Site (697) is also sourced, in part, from a vigorous ice stream that terminates in the Filchner-Ronne Ice Shelf, it may also be receiving sediment from as far away as Dronning Maud Land (Kaufman, 2016). The Site 697 record is characterized by lower sedimentation rates, which hinder how well the depocenter records the three Milankovitch periodicities (i.e. longer periodicities are favored). Unlike the Weddell Sea and Prydz Bay sites, the Wilkes Land archives are not sourced by major ice streams that terminate in ice shelves—a configuration known to accelerate ice flow. That said, wavelet analysis demonstrates obliquity governing and sedimentation rates that are within the range of Prydz Bay and the Weddell Sea localities, which could provide corroborating evidence for a dynamic East Antarctic Ice Sheet (EAIS) during the Pliocene (Cook et al., 2013; Barker, Kennett, & et al., 1988). Minor disagreement between dominating obliquity and eccentricity in the Wilkes Land well logs can likely be attributed to their distance offshore, slightly lower sedimentation rates (Table 1), and turbidite and bottom current influences (Escutia et al., 2005).

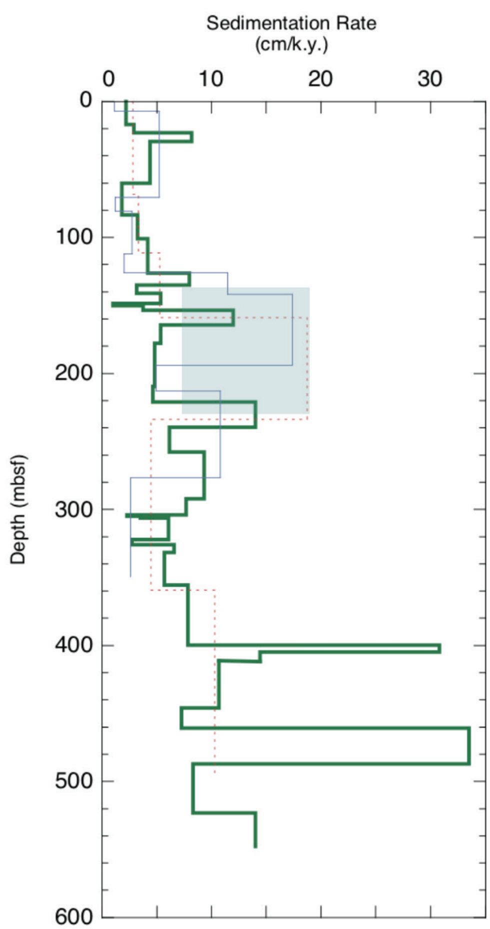

Figure 3: Independent age model (sedimentation rate versus meters below sea floor) from Bellinghausen Sea Expedition 178 Site 1095 based on paleomagnetic (dark green), radiolarian (dashed), and diatom (thin) data. Light green box indicates range of wavelet-derived sedimentation rates (cm/ kyr) for this section from gamma ray and resistivity well-log datasets, demonstrating agreement with independent geochronology. Adapted from Barker & Camerlenghi (1999).

Wavelet-derived sedimentation rates confirm accurate Milankovitch cycle assignments but also can be used in the absence of paleomagnetic and biostratigraphic age control. The mean wavelet-derived sedimentation rate for Bellingshausen Sea Site 1095 is approximately 15.8 cm/kyr, which is within the 5 to 18 cm/kyr geomagnetic, radiolarian, and diatom constraint (Fig. 3; Barker & Kennett et al., 1999). Similarly, wavelet analysis of XRF Weddell Sea cores produce a mean sedimentation rate of approximately 5.9 cm/kyr, which corresponds to an independent paleomagnetic age model suggesting 4.0 cm/kyr during the Pliocene (Barker et al., 1988). Wilkes Land well-log wavelet analysis calculates sedimentation rates that are within an order of magnitude of the well-constrained paleomagnetic, radiolarian, and diatom age model (2.5 and 4.4 cm/kyr) but still is systematically slightly overestimating. Overall, these cross-calibrated sedimentation rates exemplify the utility of wavelet analysis of continuous well-logs, such as gamma ray and resistivity, and geochemcial datasets to produce robust age control. Further cross referencing can improve the reliability of wavelet analysis in providing age models.

CONCLUSION

Both wavelet analysis and PCA provide new insights regarding how subtle geochemical and geophysical marine sediment dataset can be used to inform changes in Antarctic ice volume. We present three circum-Antarctic gamma ray and resistivity well log datasets and one split core geochemical dataset from the Weddell Sea to demonstrate ubiquitous obliquity-paced sedimentation during the Pliocene. These offshore records demonstrate that distal marine archives record orbital forcings. Linear sedimentation rates are also derived through wavelet analysis and compared with independent age models.

ACKNOWLEDGEMENTS

This material is based on work supported by the Keck Geology Consortium and the National Science Foundation under Grant No. 1659322. I would also like to acknowledge Suzanne O'Connnell, Joe Ortiz, and Will Amidon for their support. The staff at the IODP repository in Texas, especially Brian LaVey, was especially helpful with the initial data collection.

REFERENCES

Barker, P. F., Camerlenghi, A., & Acton, G. D. (1999). *Proceedings of the Ocean Drilling Program, Initial Reports* (Vol. 178).

Barker, P. ., Kennett, J. P., & et al. (Eds.). (1988). *Proceedings of the Ocean Drilling Program, 113 Initial Reports* (Vol. 113). Ocean Drilling Program. Retrieved from http://www-odp.tamu.edu/publications/113_IR/113TOC.HTM

Bentley, M. J., & Anderson, J. B. (1998). Glacial and marine geological evidence for the ice sheet configuration in the Weddell Sea–Antarctic Peninsula region during the Last Glacial Maximum. *Antarctic Science*, *10*(3), 309–325. https://doi.org/10.1017/S0954102098000388

Cook, C. P., van de Flierdt, T., Williams, T., Hemming, S. R., Iwai, M., Kobayashi, M., … Yamane, M. (2013). Dynamic behaviour of the East Antarctic ice sheet during Pliocene warmth. *Nature Geoscience*, *6*(9), 765–769. https://doi.org/10.1038/ngeo1889

Escutia, C., Santis, L., Donda, F., Dunbar, R. B., Cooper, A., Brancolini, G., & Eittreim, S. L. (2005). Cenozoic ice sheet history from East Antarctic Wilkes Land continental margin sediments. *Global and Planetary Change*, *45*, 51–81. https://doi.org/10.1016/j.gloplacha.2004.09.010

Hambrey, M. J., Ehrmann, W., & Larsen, B. (1991). Cenozoic glacial record of the Prydz Bay continental shelf, East Antarctica. In: Barron, J; Larsen, B, et al. (eds.), Proc. ODP, Sci. Results, College Station, TX. (Ocean Drilling Program), 119, 77-132, 119(10.2973/odp.proc.sr.119.200.1991), 77–132. https://doi.org/Hambrey, M. J. , Ehrmann, W. and Larsen, B. (1991)   Cenozoic glacial record of the Prydz Bay continental shelf, East Antarctica ,   In: Barron, J; Larsen, B, et al. (eds.), *Proc. ODP, Sci. Results, College Station, TX. (Ocean Drilling Program)*, *119*, 77-132, *119*, pp. 77-132.doi:10.2973/odp.proc.sr.119.200.1991 <http://doi.org/10.2973/odp.proc.sr.119.200.1991>, hdl:10013/epic.41574

Hemming, S. R. (2007). Paleoceanography, physical and chemical proxies | Terrigenous sediments. In *Encyclopedia of Quaternary Science* (pp. 1776–1785).

Kaufman, Z. (2016). Sediment interpretations of ice-rafted debris in the Weddell Sea, Antarctica: a 3-3.8 mya record from ODP Site 697. *Honors Theses - All*. Retrieved from https://wesscholar.wesleyan.edu/etd_hon_theses/1605/

Latimer, J., & Filippelli, G. (2001). Terrigenous input and paleoproductivity in the Southern Ocean. *Paleoceanography*, *16*. https://doi.org/10.1029/2000PA000586

Naish, T., Powell, R., Levy, R., Wilson, G., Scherer, R., Talarico, F., … Williams, T. (2009). Obliquity-paced Pliocene West Antarctic ice sheet oscillations. *Nature*, *458*(7236), 322–328. https://doi.org/10.1038/nature07867

Pagani, M., Lui, Z., LaRiviere, J., & Ravelo, A. C. (2010). High Earth-system climate sensitivity determined from Pliocene carbon dioxide concentrations. *Nature Geoscience. 3*(1), 27-30 https://doi.org/10.1038/ngeo724

Raymo, M., Grant, B., Horowitz, M., & H. Rau, G. (1996). Mid-Pliocene warmth: Stronger greenhouse and stronger conveyor. *Marine Micropaleontology - MAR MICROPALEONTOL*, *27*, 313–326. https://doi.org/10.1016/0377-8398(95)00048-8

Scheuer, C., Gohl, K., D. Larter, R., Rebesco, M., & Udintsev, G. (2006). Variability in Cenozoic sedimentation along the continental rise of the Bellingshausen Sea, West Antarctica. *Marine Geology*, *227*, 279–298. https://doi.org/10.1016/j.margeo.2005.12.007

Scheuer, C., Gohl, K., & Udintsev, G. (2006). Bottom-current control on sedimentation in the western Bellingshausen Sea, West Antarctica. Geo-marine letters, (10.1007/s00367-006-0019-1). https://doi.org/Scheuer, C. , Gohl, K. and Udintsev, G. (2006)   Bottom-current control on sedimentation in the western Bellingshausen Sea, West Antarctica, Geo-marine letters. doi:10.1007/s00367-006-0019-1 <http://doi.org/10.1007/s00367-006-0019-1> , hdl:10013/epic.23546

Torrence, C., & Compo, G. P. (1998). A Practical Guide to Wavelet Analysis. *Bulletin of the American Meteorological Society*, *79*(1), 61–78. https://doi.org/10.1175/1520-0477(1998)079<0061:APGTWA>2.0.CO;2

True-Alcala, T. (2015). Diffuse Spectral Reflectance-derived Pliocene and Pleistocene Periodicity from Weddell Sea, Antarctica Sediment Cores. *Honors Theses - All*. Retrieved from https://wesscholar.wesleyan.edu/etd_hon_theses/1479

Verma, K., Bhattacharya, S., Biswas, P., Shrivastava, P. K., Pandey, M., Pant, N. C., & Party, I. E. 318 S. (2014). Clay mineralogy of the ocean sediments from the Wilkes Land margin, east Antarctica: implications on the paleoclimate, provenance and sediment dispersal pattern. *International Journal of Earth Sciences*, *103*(8), 2315–2326. https://doi.org/10.1007/s00531-014-1043-4